ACTA ENTOMOLOGICA
MUSEI NATIONALIS PRAGAE
ISSN 1804-6487 (online) – 0374-1036 (print)

2024
64(2): 277–291
doi: 10.37520/aemnp.2024.019
www.aemnp.eu

RESEARCH PAPER

Anthomyza gilviventris in Palaearctic Region: integrative taxonomy, variability and habitat associations of North European population (Diptera: Anthomyzidae)

Jindřich ROHÁČEK[1,*], Sven HELLQVIST[2] & Andrea ŠPALEK TÓTHOVÁ[3]

[1] Department of Entomology, Silesian Museum, Nádražní okruh 31, 746 01 Opava, Czech Republic; ORCID:0000-0003-3311-2087
[2] Älvtået 4, 903 60 Umeå, Sweden; e-mail: shellq@telia.com
[3] Department of Botany and Zoology, Faculty of Science, Masaryk University, Kotlářská 2, CZ-611 37 Brno, Czech Republic; e-mail: tothova@sci.muni.cz
[*] corresponding author: e-mail: rohacek@szm.cz

Accepted:
11th September 2024

Published online:
31st October 2024

Abstract. *Anthomyza gilviventris* Roháček & Barber, 2016, hitherto known only from the Nearctic Region, is recorded from the Palaearctic Region (NE Sweden) for the first time. Specimens from the Swedish population have been compared with those of *A. gilviventris* from Canada and the USA and those of *A. tschirnhausi* Roháček, 2009 from the Kamchatka Peninsula (Far East of Russia). Both morphological and molecular analyses (BI and RAxML, based on seven DNA markers: 12S, 16S, 28S, COI, COII, CytB, ITS2) confirmed that the Swedish specimens belong to *A. gilviventris*. Because no specimen of *A. tschirnhausi* has been available for molecular study, the most diagnostic morphological characters used for separation of this species from *A. gilviventris* have been re-evaluated with respect to Swedish specimens, and their variability discussed. However, these differences, although stable, are relatively small and, consequently, the possibility that they fall within the limits of a single variable species has not been entirely eliminated. New biological information (habitat and host-plant associations) on the Swedish population of *A. gilviventris* is presented.

Key words. Diptera, Anthomyzidae, *Anthomyza tschirnhausi* group, biology, distribution, DNA sequences, morphology of terminalia, taxonomy, Sweden, Palaearctic Region

Zoobank: http://zoobank.org/urn:lsid:zoobank.org:pub:04DCFDED-513A-423D-BDBF-F41CFCB2728C
© 2024 The Authors. This work is licensed under the Creative Commons Attribution-NonCommercial-NoDerivs 3.0 Licence.

Introduction

Anthomyza gilviventris Roháček & Barber, 2016 has been described from the Nearctic Region as a relatively common and widespread species. It is a member of *Anthomyza* Fallén, 1810, currently the most speciose genus of the family Anthomyzidae. Roháček & Barber (2016) classified it within the *Anthomyza tschirnhausi* group, together with *A. tschirnhausi* Roháček, 2009 (only known from Kamchatka, Far East of Russia) and *A. shewelli* Roháček & Barber, 2016 (widespread in eastern North America). The *Anthomyza tschirnhausi* group is distinguished by a number of apomorphic features including very distinctive modifications of the male and female terminalia (for detail see Roháček & Barber 2016: 277–278). On the other hand, all three species of this group are very similar, closely related and, moreover, unusually variable, at least as regards both Nearctic species. Consequently, their identification can be difficult, particularly with respect to atypical dark forms known in both *Anthomyza shewelli* and *A. gilviventris* (see Roháček & Barber 2016). The East Palaearctic *A. tschirnhausi*, known from only a few specimens (Roháček 2009: 48), very closely resembles a dark form of *A. gilviventris*. Roháček et al. (2019) presented a molecular hypothesis of the phylogenetic relationships of the genus *Anthomyza* and allied genera based on seven mitochondrial and nuclear gene markers, that included both Nearctic species, namely *A. shewelli* and

A. gilviventris. The distinctness and validity of both these species were confirmed by molecular data as was also the sister-group relationship of the *A. tschirnhausi* group and the *A. gracilis* group.

In 2016, one of us (SH) discovered in NE Sweden (Ångermanland) the first specimens of the *A. tschirnhausi* group from the West Palaearctic area. Although they most closely resembled those of the Nearctic *A. gilviventris*, there were two other possible species identities: they could represent a (previously unknown) pale form of *A. tschirnhausi*, or they could belong to an unnamed species. Additional collecting effort (by SH) in 2017 yielded a good series of specimens from two localities thus providing the opportunity for further morphological and molecular investigation. Results of these studies are presented below.

Material and methods

Material. Apart from *Anthomyza gilviventris* specimens (20 ♂♂ and 27 ♀♀) from Sweden (for their data see below), numerous paratypes of *A. gilviventris* and *A. shewelli* from Canada deposited in SMOC (for their data see Roháček & Barber 2016) and also part of the type material of *A. tschirnhausi* (including the holotype male in IAES and paratypes in SMOC, see Roháček 2009: 48) have been examined. Acronyms of collections are as follows:

IAES	Institute of Agricultural and Environmental Sciences, Estonian Agricultural University, Tartu, Estonia;
NHRS	The Swedish Museum of Natural History, Stockholm, Sweden;
SHU	Sven Hellqvist private collection, Umeå, Sweden;
SMOC	Silesian Museum, Opava, Czech Republic.

The material from Sweden was originally preserved in ethanol but the majority of specimens were dried and mounted on minuten pins or on triangular pinned paper points during the course of this analysis. Only some (including bodies of those used for molecular work) are preserved in glycerine in pinned plastic microvials. Abdomens of a number of specimens were detached, cleared by boiling for several minutes in a 10% solution of potassium hydroxide (KOH) in water, then neutralized in a 10% solution of acetic acid (CH3COOH) in water, washed in water and subsequently transferred to glycerine. Postabdominal structures were dissected and examined in a drop of glycerine under binocular microscopes (Reichert, Leica S9i). Detailed examinations of genitalic structures were performed with a compound microscope (JENAVAL). After examination, all dissected parts were put into small plastic tubes containing glycerine, sealed with hot forceps and pinned below the respective specimens.

Drawing techniques and photography. Details of the male terminalia were drawn by JR by means of Abbe's drawing apparatus on a compound microscope (JENAVAL) at larger magnification (130–500×). Whole adult specimens (male and female, dried and minuten-pinned) were photographed by Mikael Marberg (Umeå) by means of a Canon EOS Kiss X3 camera with a Canon MP-E65 macro lens. Photos were stacked using Helicon focus software and images thereafter processed in Adobe Photoshop CS.

Molecular analyses. ***Taxon sampling.*** The analysed dataset contains 67 species (64 Anthomyzidae + 3 outgroup taxa). All taxa for which specimens are available for DNA extraction are included in the molecular analysis. Except for four additions (3 specimens of *Anthomyza gilviventris* from Sweden and an additional specimen of *A. shewelli* from Canada: Ontario), they are listed in full (with names, authors and source localities of analysed specimens) in Roháček et al. (2019: table 1, most species), Barber & Roháček (2020: table 1, species of *Carexomyza* Roháček, 2009 only) and Roháček & Tóthová (2021: table 1, *Mumetopia interfeles* Roháček, 2021 and *Stiphrosoma stylatum* Roháček & Barber, 2005). We used one specimen per species except for an unnamed species of the *Mumetopia nigrimana* group and *Anthomyza shewelli*, both of which we processed two specimens, and *Anthomyza gilviventris*, of which we used four specimens. The outgroup included *Geomyza tripunctata* Fallén, 1823 and *Opomyza florum* (Fabricius, 1794) (Opomyzidae, the sister family of the Anthomyzidae, cf. Roháček 1998, 2006, Lonsdale 2020), and *Clusia flava* (Meigen, 1830) (Clusiidae, formerly considered to be the most generalized family of the Opomyzoidea, cf. McAlpine 1989 but see Lonsdale 2020) which was used to root the phylogenetic trees.

DNA extraction, PCR and sequencing. The adult flies used for analysis were air-dried or ethanol-preserved. The molecular procedures and protocols are fully documented in Roháček et al. (2019). GenBank accession numbers

Table 1. Specimens of the *Anthomyza tschirnhausi* group in our dataset of Anthomyzidae used for the molecular analyses, with their GenBank accession numbers.

Species	Locality	12S	16S	COIa	COIb	COII	CytB	28S	ITS2
A. gilviventris CDN	Canada (Ontario)	MH727106	MH727125	MH729932	MH729946	MH729956	MH742388	MH727144	MH727162
A. gilviventris S1	Sweden	PP504660	PP504505	PP457625	PP457629	PP475157	PP475159	PP504499	PP504657
A. gilviventris S2	Sweden	PP504661	PP504506	PP457626	PP457630	–	–	PP504500	–
A. gilviventris S3	Sweden	PP504662	PP504507	PP457627	PP457631	PP475158	–	PP504501	PP504658
A. shewelli CDN1	Canada (Ontario)	MH727105	MH727124	–	–	MH729955	MH742387	MH727143	MH727161
A. shewelli CDN2	Canada (Ontario)	PP504663	PP504508	PP457628	–	–	–	PP504502	PP504659

for the sequences are listed in Roháček et al. (2019: table 1), Barber & Roháček (2020: table 1) and Roháček & Tóthová (2021: table 1), so only those of the species of the *Anthomyza tschirnhausi* group are given here (Table 1).

Alignment and phylogenetic analyses. All the sequences were aligned using MAFFT version 7 (Katoh & Standley 2013) on the MAFFT server (http://mafft.cbrc.jp/alignment/server/). Alignment protocols are fully outlined in Roháček et al. (2019). The final dataset consisted of 72 specimens as terminal "taxa" (67 species) and 4568 characters: 12S – 349 bp, 16S – 361 bp, 28S – 614 bp, COI – 1248 bp, COII – 633 bp, CytB – 646 bp, ITS2 – 717 bp. The dataset was analyzed using maximum likelihood (ML) and Bayesian inference (BI) methods. The analyses were conducted on the CIPRES computer cluster using Mr Bayes v. 3.2.7. (Ronquist et al. 2012) and RAxML v.8 (Stamatakis 2014). The node support values are given with the posterior probability (PP) above the nodes (if value > 0.5) and the bootstrap value (BV) below the nodes in the resulting tree depicted in Fig. 42. For the BI, all parameters were unlinked across partitions. The convergence of the runs was assessed by checking the potential scale reduction factor (PSRF) values of each parameter (in all cases, approaching 1.000) and the standard deviation of split frequencies (< 0.01). The mean log-likelihood value for the best-fit BI tree was -43973.63, for the ML tree it was -45502.526652. The resulting phylogenetic tree (consensus tree) was visualized using Interactive Tree Of Life (iTOL; Letunic & Bork 2016).

The genetic distances of the barcoding region of COI of *Anthomyza gilviventris* and of *A. shewelli* specimens were calculated in MEGA version 11 (Tamura et al. 2021) using the Kimura 2-parameter (K2P) model and are presented in Table 2.

Morphological terminology. The terminology follows that used in monographs of Anthomyzidae by Roháček (2006) and/or Roháček & Barber (2016) including terms of the male hypopygium and female terminalia. For male genitalia terminology, the "hinge" hypothesis of the origin of the eremoneuran hypopygium (see Zatwarnicki 1996) has been adopted. The following synonymous terms of the male genitalia emanating from other hypotheses and used in recent manuals of Diptera (Cumming & Wood 2009, 2017) and/or the monograph of Griffiths (1972) need to be listed (terms used here first): aedeagus = phallus; ejacapodeme = ejaculatory apodeme; epandrium = periandrium; gonostylus = surstylus; medandrium = bacilliform sclerite, intraepandrial or intraperiandrial sclerite; phallapodeme = aedeagal apodeme; postgonite = gonite, paramere. Morphological terms of the male terminalia are depicted in Figs 3, 6, 14, and those of the female on Figs 36, 39.

Figs 1–2. *Anthomyza gilviventris* Roháček & Barber, 2016, adult habitus (Sweden). 1 – male, laterally; 2 – female, laterally. Scale bar: 0.5 mm. Photo by M. Marberg.

Results

Anthomyza gilviventris Roháček & Barber, 2016

(Figs 1, 2, 4–7, 10–13, 16–22, 25–31, 33–35, 37, 38, 40, 41)

New material examined. SWEDEN: Ångermanland: Bjurholm parish: river Lögdeälven, at the outlet of the stream Mossavattsbäcken, 64°2′24″N, 18°44′50″E, [river shore, sweeping], 2.vii.2016, 1 ♂ 3 ♀♀ (SMOC, SHU), 26.vii.2016, 1 ♀ (SMOC); same locality, river shore, [sweeping] on *Carex rostrata* and *C. acuta*, 8.vii.2017, 1 ♂ 1 ♀ (NHRS, SHU), 15.vii.2017, 12 ♂♂ 15 ♀♀ (NHRS, SMOC, SHU, including 3 ♂♂ 3 ♀♀ genit. prep., plus 1 ♂ 2 ♀♀ used for molecular study,); Bjurholm parish: river Öreälven at Lagnäset, 63°54′58″N, 19°12′40″E, river shore, [sweeping] on *Carex rostrata*, 15.vii.2017, 6 ♂♂ 4 ♀♀ (SMOC, SHU, 3 ♂♂ 1 ♀ genit. prep.); Västerbotten: Vindeln commune: Lerfallet, 64°21′41″N, 19°32′19″E, along a small creek, probably on *Carex acuta*, 7.vii.2021, 2 ♀♀ (SHU), all Sven Hellqvist leg.

Morphological analysis. ***Male.*** The comparative morphology in the male sex (Fig. 1) has been focused on characters of the male genitalia considered by Roháček & Barber (2016) to best distinguish *A. gilviventris* and *A. tschirnhausi*. These mainly include (1) the shape of the epandrium (in caudal view), (2) the form of the anal fissure, (3) the shape and sclerotization of the transandrium and its caudal process, (4) the armature of the apex of the filum of the distiphallus, and, particularly (5) the armature of the saccus of the distiphallus. In addition, the shape and chaetotaxy of the gonostylus has also been compared in both species (including specimens from the Swedish population).

Epandrium. The epandrium (in caudal view) proved to be narrower and dorsally more tapered in *A. gilviventris* (Fig. 4) than in *A. tschirnhausi* (Fig. 3). In Swedish male specimens (see Figs 5–7), the epandrium shape more closely resembles that of the epandrium in *A. gilviventris* specimens from Canada and the USA.

Anal fissure. Also, the anal fissure of the epandrium is distinctly narrow in *A. gilviventris* (Fig. 4) while in *A. tschirnhausi* (Fig. 3) it is more broadened ventrally. Although the shape of the anal fissure was found to be rather variable in Swedish specimens (see Figs 6–7), it was never as wide as that of *A. tschirnhausi* and, consequently, their anal fissure proved to be more similar to that of Nearctic specimens.

Transandrium and caudal process. These structures should be narrower in *A. gilviventris* as suggested by Roháček & Barber (2016). Although illustrations of a typical specimen of *A. gilviventris* from Canada: Ontario (Roháček & Barber 2016: fig. 491) and of a paratype of *A. tschirnhausi* from Kamchatka (Roháček 2009: fig. 62) indicate distinct differences, the widths of both the transandrium and its caudal process are, in fact, variable and most specimens from Sweden proved to be rather intermediate between both these extremes. Moreover, these structures can hardly be used for practical identification inasmuch as this posterior part of the hypandrial complex is difficult to correctly prepare to be precisely comparable in all specimens examined.

Filum apex. The apex of the filum of the distiphallus seems to be differently spinose with *A. gilviventris* having a number (usually > 10) of small subterminal spines (see Figs 13, 16) while that of *A. tschirnhausi* bears only 3 of them (Figs 8, 9). The Swedish specimens have the terminal part of the filum variously spinose (Figs 10–12) and, rather surprisingly, bearing only 4–7 small spines thus differing in this respect from the Nearctic specimens. On the other hand, the apical part of the filum of the male holotype of *A. tschirnhausi* has only 3 (very minute) spines (apart from the two forming the bicuspid end on the apex, Fig. 8), thus less than have specimens from Sweden. It also should be stressed that both *A. gilviventris* and *A. tschirnhausi* have the apex of the filum finely bicuspid (Figs 8–13) although this fact was not given in the original description of the latter species (see Roháček 2009: 50). The extent and number of spinulae covering most of the filum, previously considered to be clearly greater in *A. gilviventris* than in *A. tschirnhausi* (cf. Figs 9 and 13), have been found variable, ranging from relatively sparse to numerous in both Nearctic (usually more numerous, Figs 13, 16) and Swedish populations (usually sparser, Figs 10–12, 17) of *A. gilviventris* but also in *A. tschirnhausi* (the least numerous, see Figs 8, 9).

Saccus. The distal membranous part of the saccus of the distiphallus is armed with some spines in the terminal part. Their number is somewhat variable as found by Roháček & Barber (2016) for *A. gilviventris* with 5–8 (most frequently 5, cf. Fig. 16) distal spines. The same variability has also been confirmed in the specimens from the Swedish population where 5–7 spines near the apex of the saccus have been documented (Figs 17–22). In *A. tschirnhausi*, the saccus has been supposed to bear only 3 terminal spines (Fig. 14) (see also Roháček 2009) but re-examination of the male holotype revealed that there could also be 4 such spines (Fig. 15). Nevertheless, this number remains less than the minimum number of spines in *A. gilviventris*. More importantly, we have found that the single spine near the base of the membranous part of the saccus (see Figs 16–22) occurring in *A. gilviventris* (including all Swedish male specimens) is wholly absent in *A. tschirnhausi* (also confirmed in the holotype, Fig. 15) while it is present in the other Nearctic species, *A. shewelli*, see Roháček & Barber (2016: 289).

Gonostylus. Roháček & Barber (2016) found that the shape and chaetotaxy of the gonostylus are variable in both Nearctic species, viz., *A. gilviventris* and *A. shewelli*. Despite this variability, the general outline (in largest extension view) of the gonostylus is distinctly different in these two species, mainly in the curvature of its anterior margin (convex in *A. shewelli*, concave to straight in *A. gilviventris*). Because the formation and setosity of the gonostylus are normally species-specific characters in Anthomyzidae, we attempted to find differences in the gonostylus also in Palaearctic *A. gilviventris* and *A. tschirnhausi*. However, examination of the gonostylus of specimens from Sweden (Figs 29–31) and comparison with those of *A. gilviventris* specimens from the Nearctic Region (Figs 25–28) and those of *A. tschirnhausi* from Kamchatka (Figs 23, 24) has not revealed any clear differences. Also, the extent of the micropubescence and chaetotaxy of the inner side of the gonostylus proved to be variable and overlapping in both species, including within the Swedish population of *A. gilviventris*.

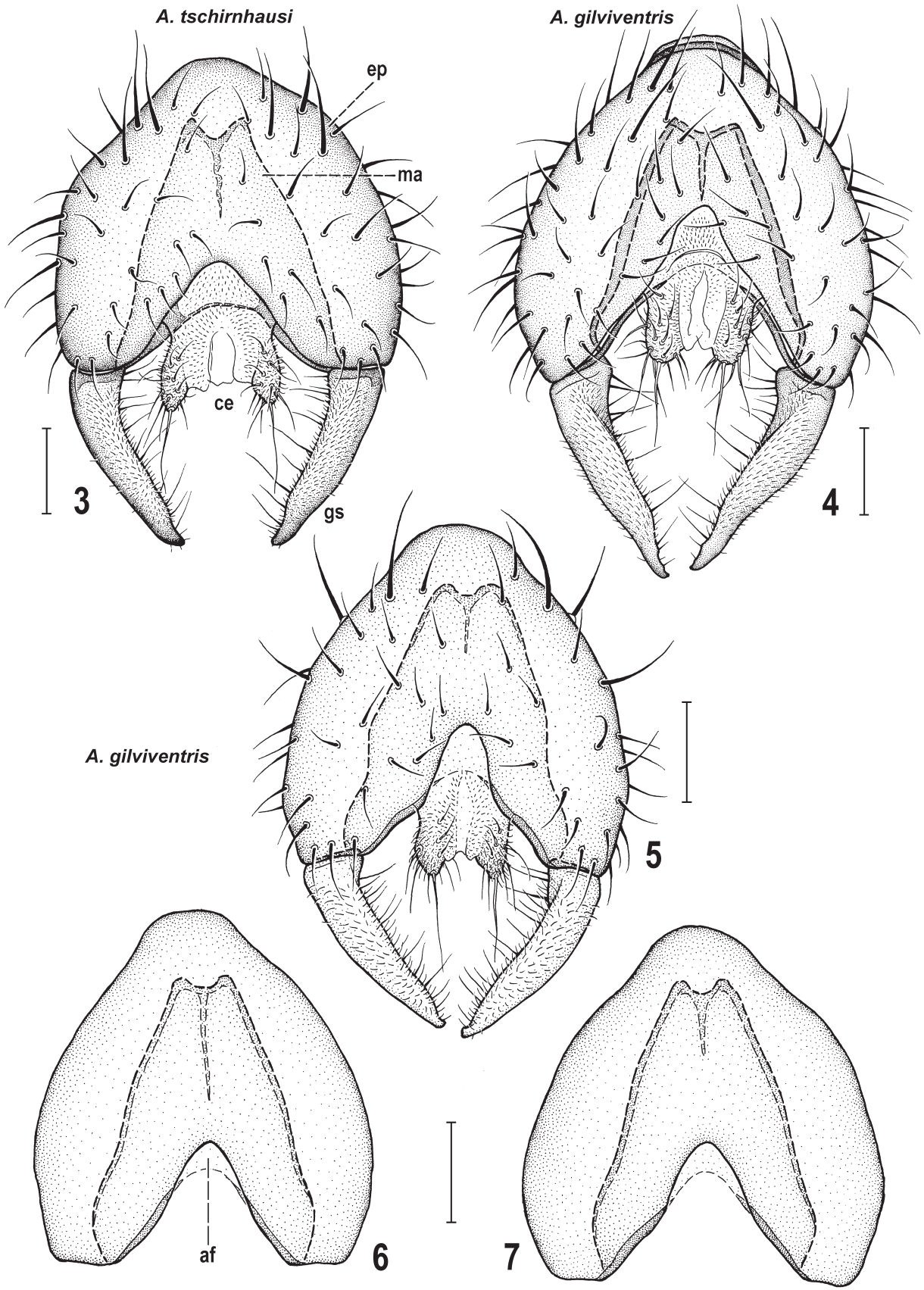

Figs 3–7. *Anthomyza* species, male external genitalia (3–5) or epandrium (6, 7), caudally. 3 – *A. tschirnhausi* Roháček, 2009, paratype (Kamchatka); 4–7 – *A. gilviventris* Roháček & Barber, 2016: 4 – paratype, Ontario; 5 – Sweden: Lögdeälven; 6, 7 – Sweden: Öreälven. Scale bars: 0.1 mm. Abbreviations: af – anal fissure, ce – cerci, ep – epandrium, gs – gonostylus, ma – medandrium. Fig. 3 adapted from Roháček (2009: fig. 58), Fig. 4 from Roháček & Barber (2016: fig. 487).

Female. Examination of females (Fig. 2) from Sweden revealed that they are (including characters of postabdomen) practically identical with the Nearctic specimens of the typical (= yellow) form of *A. gilviventris.* The narrow subterminal darkening of the female T7+S7 (best visible in Fig. 41 but also in abdomen of dried specimens, see Fig. 2) commonly occurs in the Nearctic specimens with a yellow abdomen (cf. Roháček & Barber 2016: fig. 484) but it can be absent in the lightest specimens having T7+S7 posteriorly almost entirely yellow (Figs 37, 40). According to Roháček & Barber (2016), females of *A. tschirnhausi* differ from those of *A. gilviventris*, apart from the darker abdomen, also by (1) the shape and surface structure of the spermathecae, (2) the shape of T7+S7, (3) the shape of T8 and (4) the shape of S8. However, both species also differ in the shape of sclerites of the 10th abdominal segment (T10, S10) as recognized below.

Spermathecae. In *A. tschirnhausi* females, the spermathecae are elongately ellipsoid having denser striae covering a larger part of their surface (see Fig. 32), in contrast to those of *A. gilviventris* which are broadly suboval with sparser striae (Figs 34, 35). The latter, more broad, type of spermathecae has also been found in females from Sweden (see Fig. 33).

Tergosternum T7+S7. Females of *A. gilviventris* have T7+S7 more strongly tapered posteriorly (Figs 37, 40) than have females of *A. tschirnhausi* (Figs 36, 39). Swedish females have this tergosternum also strongly narrowed posteriorly, thus very similar to that of Nearctic *A. gilviventris*, see Figs 38, 41).

Abdominal tergum T8. In *A. gilviventris*, T8 is extremely long, slender (narrowest at about the middle) and relatively dark-pigmented as seen in both Nearctic (Fig. 37) and Swedish specimens (Fig. 38). Females of *A. tschirnhausi* also have T8 elongate and narrowed but it is distinctly wider, not further narrowing in the middle, and has paler pigmentation (Fig. 36).

Abdominal sternum S8. This sclerite is longitudinally divided into two sclerites as in other *Anthomyza* species but is markedly elongate and without micropubescence in all species of the *A. tschirnhausi* group. However, in *A. gilviventris* it is more slender and longer than in all other relatives (Fig. 40) as also seen in Swedish specimens (Fig. 41). In contrast, *A. tschirnhausi* has both parts of the female S8 distinctly the shortest and widest of all species of the group (Fig. 39), hence different from those of *A. gilviventris*. Thus, the Swedish females agree with typical females of *A. gilviventris* from the Nearctic Region in all postabdominal characters treated above.

10th abdominal segment. Both sclerites of this segment are markedly more elongate in *A. gilviventris* (for T10 see Figs 37, 38; for S10 see Figs 40, 41) than in *A. tschirnhausi* (Figs 36, 39). Moreover, T10 of *A. gilviventris* normally has some smaller setae in addition to the medial pair of

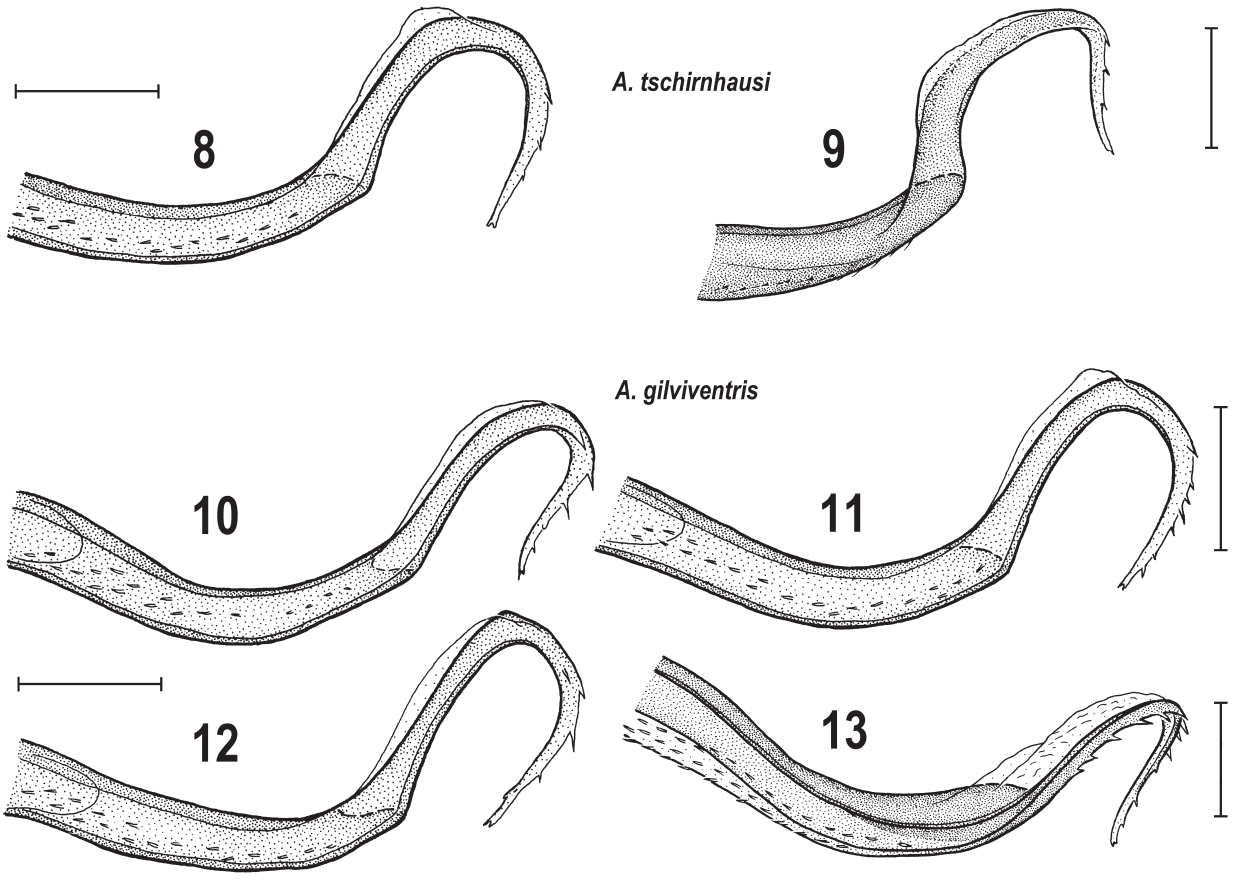

Figs 8–13. *Anthomyza* species, males, apex of filum of distiphallus, subventrally. 8–9 – *A. tschirnhausi* Roháček, 2009: 8 – holotype (Kamchatka), 9 – paratype (Kamchatka). 10–13 – *A. gilviventris* Roháček & Barber, 2016: 10, 11 – Sweden: Öreälven; 12 – Sweden: Lögdeälven; 13 – paratype, Ontario. Scale bar: 0.05 mm. Fig. 9 adapted from Roháček (2009: fig. 59), Fig. 13 from Roháček & Barber (2016: fig. 488).

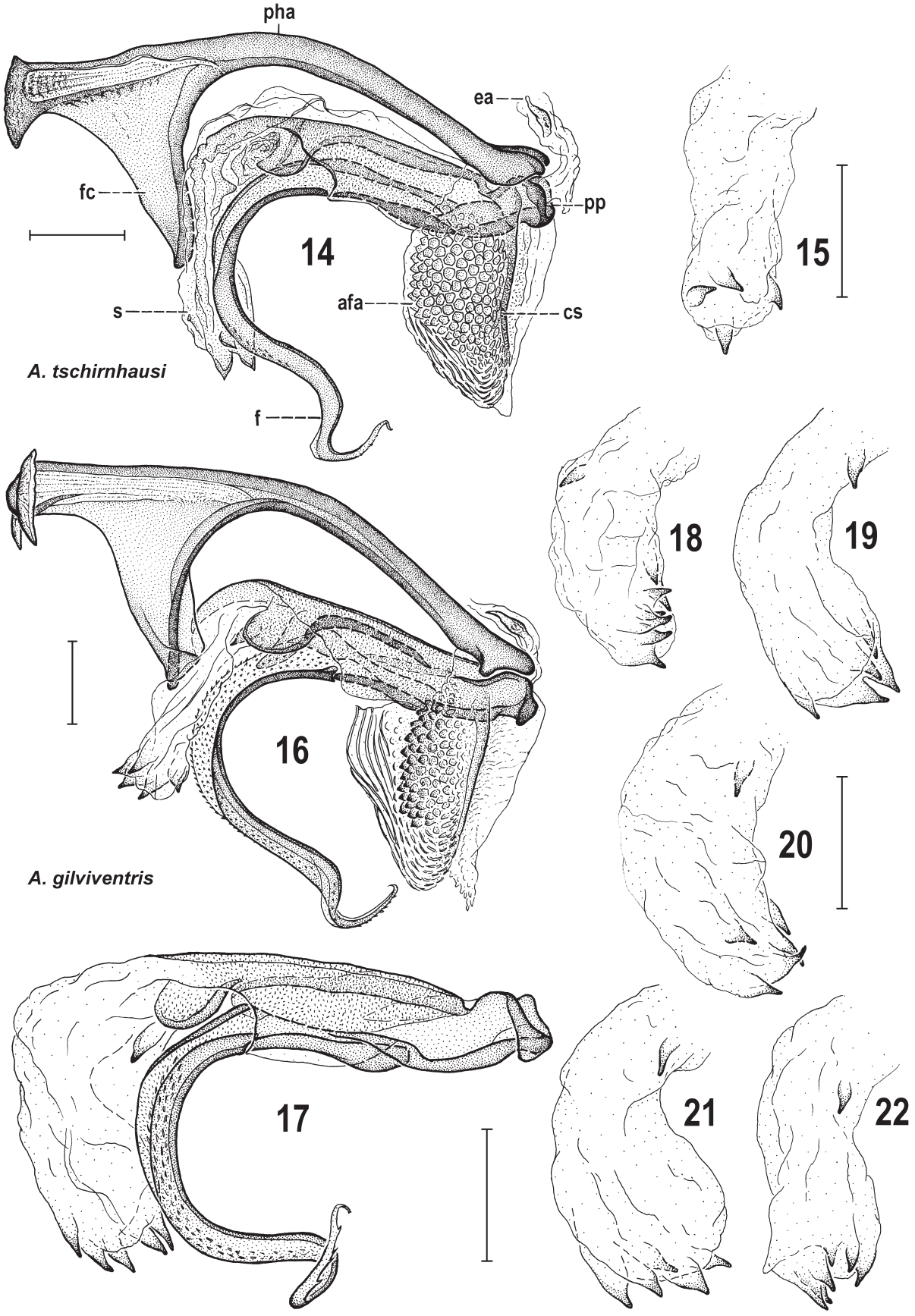

Figs 14–22. *Anthomyza* species, males, aedeagal complex (14, 16), distiphallus (17) or saccus of distiphallus (others), left laterally. 14–15 – *A. tschirnhausi* Roháček, 2009: 14 – paratype (Kamchatka); 15 – same species, holotype (Kamchatka). 16–22 – *A. gilviventris* Roháček & Barber, 2016: 16 – paratype, Ontario; 17, 21, 22 – Sweden: Lögdeälven; 18, 19, 20 – Sweden: Öreälven. Scale bars: 0.1 mm. Abbreviations: afa – aedeagal part of folding apparatus, cs – connecting sclerite, ea – ejacapodeme, f – filum of distiphallus, fc – fulcrum, pha – phallapodeme, pp – phallophore, s – saccus of distiphallus. Fig. 14 adapted from Roháček (2009: fig. 61), Fig. 16 from Roháček & Barber (2016: fig. 492).

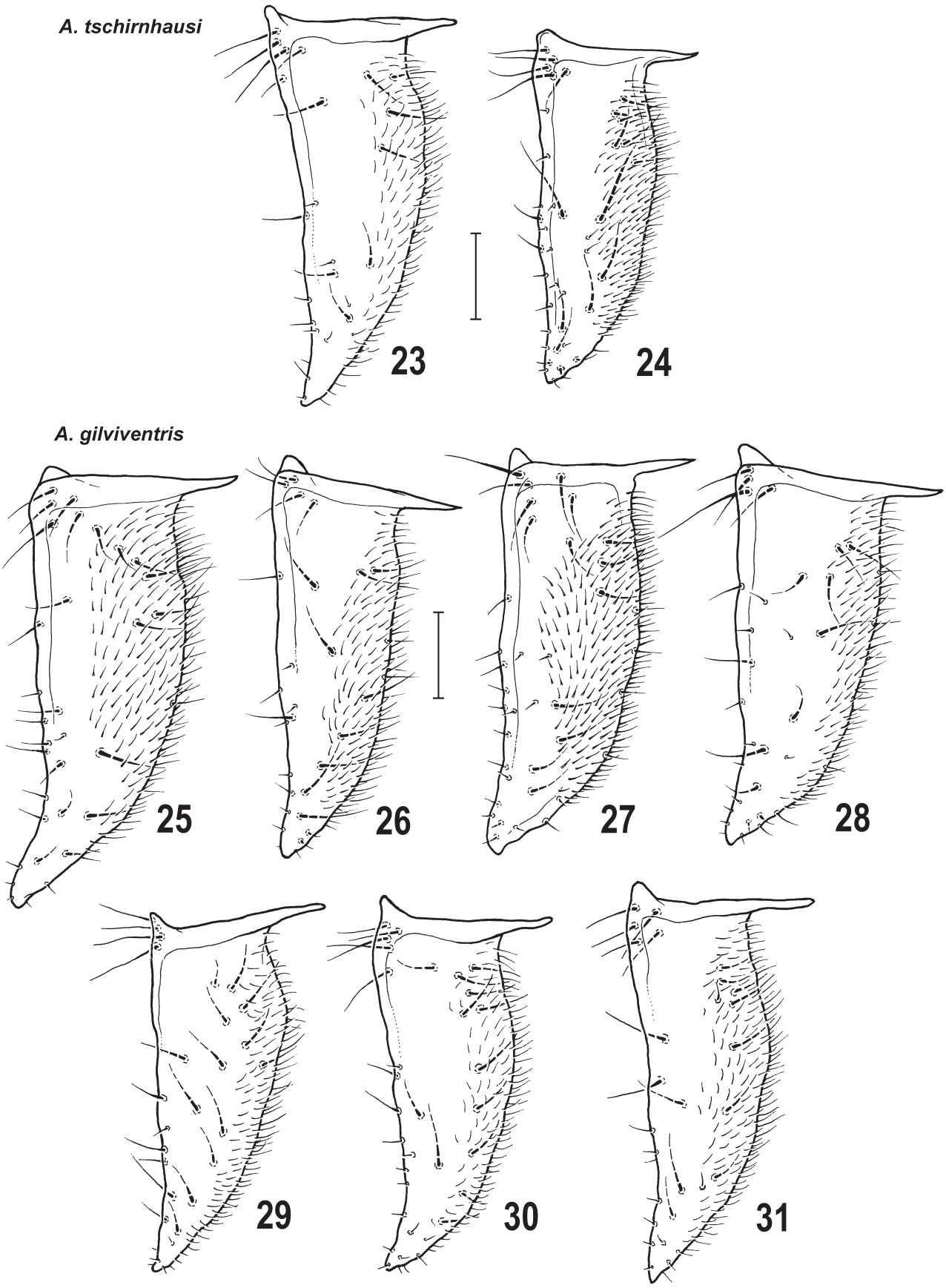

Figs 23–31. *Anthomyza* species, males, gonostylus, ventrolaterocaudally (widest extension). 23–24 – *A. tschirnhausi* Roháček, 2009: 23 – holotype, Kamchatka; 24 – paratype, Kamchatka; 25–31 – *A. gilviventris* Roháček & Barber, 2016: 25 – paratype, British Columbia; 26, 27 – paratypes, Colorado; 28 – paratype, Ontario; 29 – Sweden: Lögdeälven; 30, 31 – Sweden: Öreälven. Scale bars: 0.05 mm. Fig. 23 adapted from Roháček (2009: fig. 57), Figs 25–28 from Roháček & Barber (2016: figs 510, 511, 493, 512).

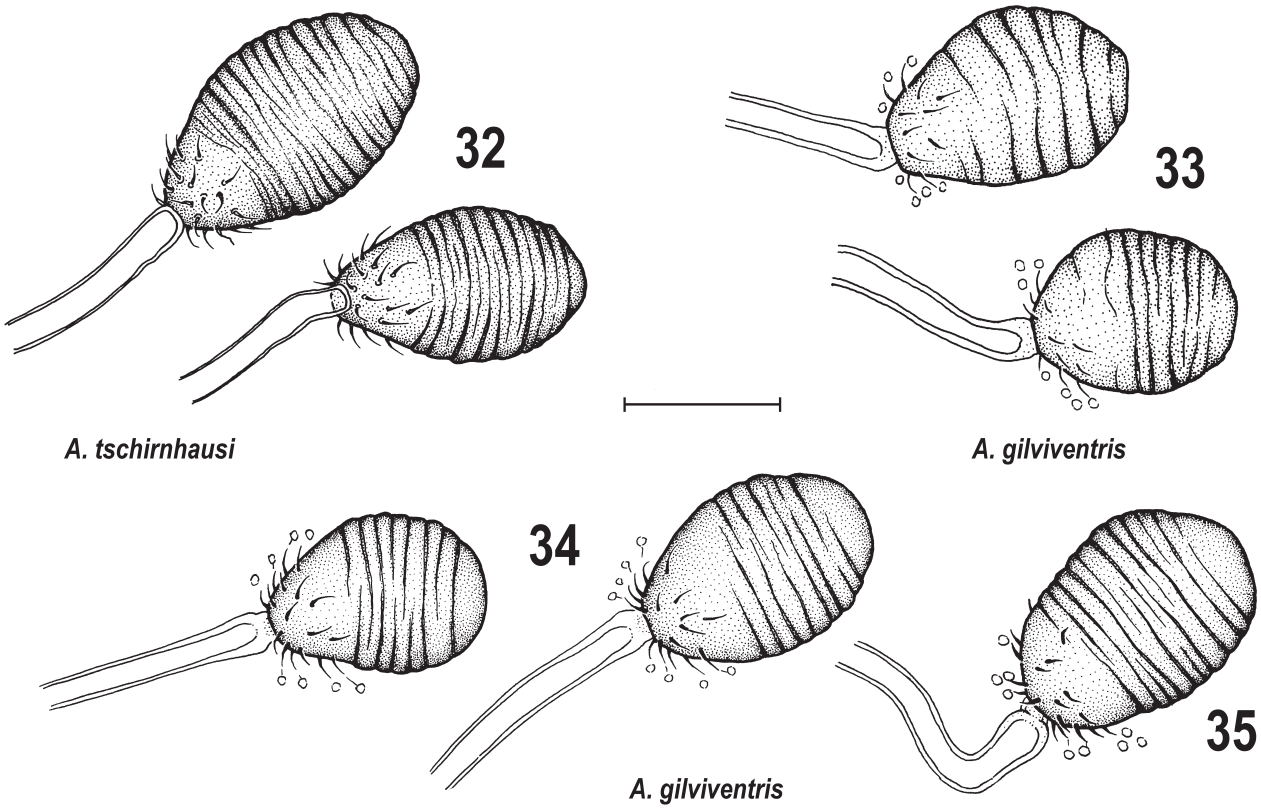

Figs 32–35. *Anthomyza* species, females, spermathecae. 32 – *A. tschirnhausi* Roháček, 2009, paratype (Kamchatka); 33–35 – *A. gilviventris* Roháček & Barber, 2016: 33 – Sweden: Lögdeälven; 34 –paratype, Ontario; 35 – paratype, Colorado, dark form. Scale bars: 0.05 mm. Membranous minute globules at apices of spines not illustrated in Fig. 32. Fig. 32 adapted from Roháček (2009: figs 66 (mirrored), 67), Figs 34, 35 from Roháček & Barber (2016: figs 494, 498, 514).

longer setae (Figs 37, 38). We have also found that specimens from Sweden have T10 distinctly narrower (Fig. 38) than specimens from Canada (Fig. 37) indicating certain differences between populations in N. Europe and N. America (as does the differently spinose apex of the filum of the distiphallus as described above).

Molecular analysis. ***Affinity of the Swedish specimens.*** We tested the relationships of the specimens from the Swedish population by means of both the Bayesian inference (MrBayes) and the maximum likelihood (RAxML) hypotheses. In both methods, all three specimens from Sweden were clustered together (see Fig. 42) and this cluster was resolved as a sister clade of the *Anthomyza gilviventris* specimen from Canada (Ontario). *Anthomyza shewelli*, represented by two specimens (both also from Ontario) in our dataset, is the only other species of the *A. tschirnhausi* group analysed. With the addition of specimens (of both species) to these analyses, *A. shewelli* is again recognized as a sister species of *A. gilviventris*, and consequently, their topology, as recognized by previous molecular hypotheses (Roháček et al. 2019), has been confirmed. However, because of the absence of fresh material of *A. tschirnhausi* from Kamchatka, it has not been possible to study its relationships by means of the above molecular methods. Inasmuch as this species was found to be the closest relative of *A. gilviventris* by means of the analysis of morphological characters (see above and also in morphological hypothesis by Roháček & Barber 2016: fig. 605), it can be presupposed that *A. gilviventris* is also genetically closer (if not conspecific with it) to *A. tschirnhausi* than to *A. shewelli*. This question can only be resolved in the future, as and when specimens of *A. tschirnhausi* become available for molecular study.

Relationships of the A. tschirnhausi group. This group, represented by *A. gilviventris* and *A. shewelli* in our dataset, has been confirmed as the sister group of the *A. gracilis* group with high support. This is in full agreement with both previous morphological (Roháček & Barber 2016) and molecular (Roháček et al. 2019) phylogenetic hypotheses.

Barcoding of the species of the A. tschirnhausi group. The comparison of COI sequences of *A. gilviventris* specimens from Sweden and Canada and of *A. shewelli* specimens from Canada found that their pairwise genetic distances are relatively small (see Table 2). Distances of COI among specimens of *A. gilviventris* range from 0.0 to 0.5%, with the differences between Canadian and Swedish specimens being greater (0.4–0.5%) than among specimens from the Swedish population (0.0–0.2%). This indicates that the populations in Europe (Sweden) and N. America (Canada) are somewhat different. On the other hand, the distances of COI between *A. gilviventris* and *A. shewelli* specimens proved to be distinct though relatively small (2.2–3.0%) with, interestingly, the smallest distance occurring between Canadian specimens (2.2%).

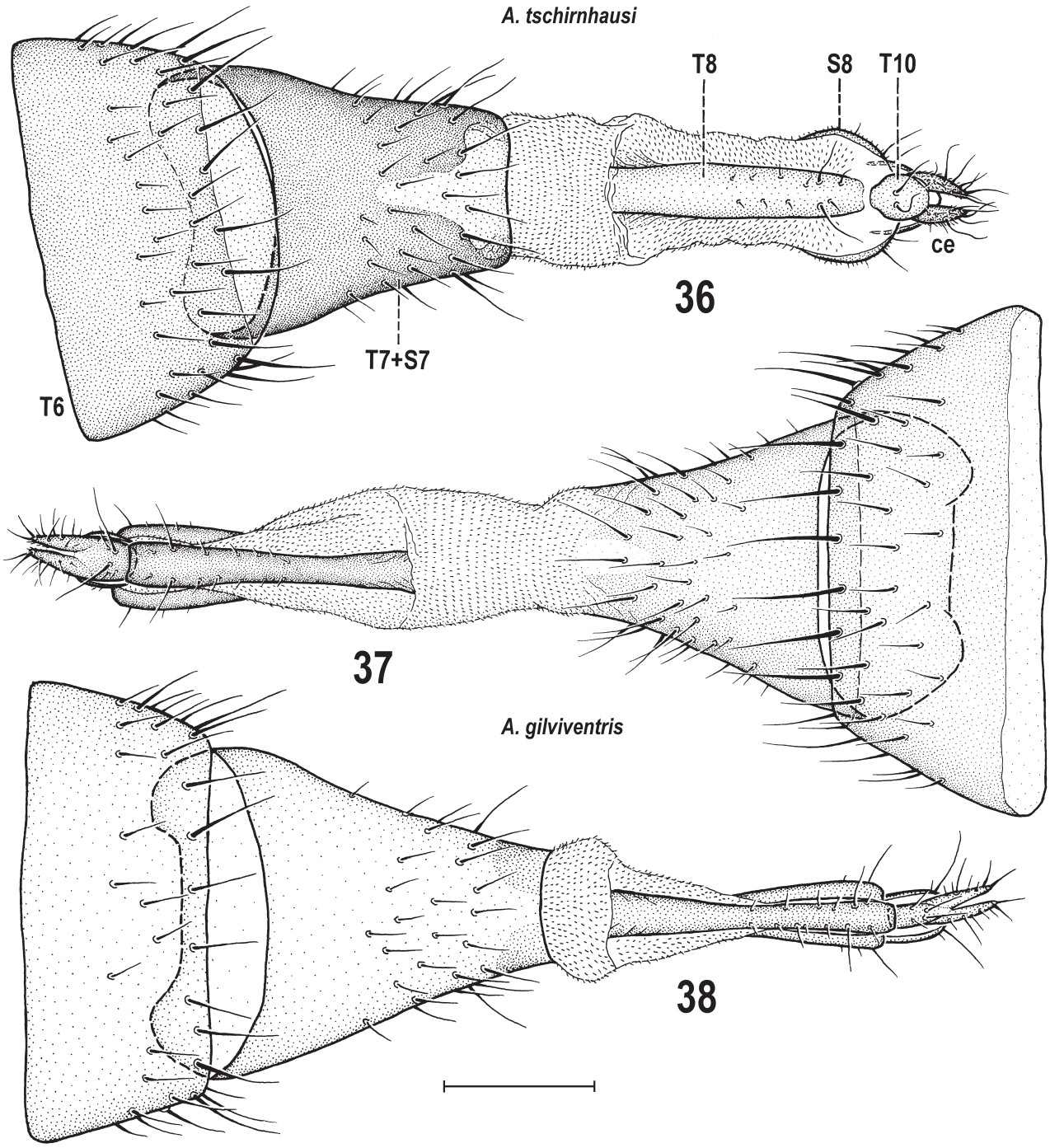

Figs 36–38. *Anthomyza* species, females, postabdomen dorsally. 36 – *A. tschirnhausi* Roháček, 2009, paratype (Kamchatka); 37–38 – *A. gilviventris* Roháček & Barber, 2016: 37 – paratype, Ontario; 38 – Sweden: Lögdeälven. Scale bar: 0.2 mm. Abbreviations: ce – cerci, S – sternum, T – tergum, T7+S7 – tergosternum 7. Fig. 36 adapted from Roháček (2009: fig. 63), Fig. 37 from Roháček & Barber (2016: fig. 495, mirrored).

Biology. In the Nearctic Region, *A. gilviventris* mainly inhabits various wetland habitats, particularly those with sedges (*Carex* and *Scirpus* species, see Roháček & Barber 2016) which may be host plants of this anthomyzid fly. Most frequently, *Carex utriculata* and *Scirpus microcarpus* have been encountered as dominant graminoids in the habitats where *A. gilviventris* commonly occurs, but this species was also found in growths of several other sedges (e.g. *Carex aquatilis*, *C. stipata*) often intermixed with *Equisetum fluviatile*.

In Sweden, adults of *A. gilviventris* have been mainly collected on the shores of rivers (Fig. 43), all specimens in July (in Ontario adults of this species occur in May to September, see Roháček & Barber 2016).

Although various *Carex* species were swept at the Lögdeälven river locality, *A. gilviventris* specimens were found only in *C. rostrata* (4 ♂♂ 11 ♀♀) and *C. acuta* (8 ♂♂ 4 ♀♀) growing on the river shore (on July 15, 2018). The river bank is rather narrow and stony here, with *C. rostrata* growing in the water (intermixed with *Equisetum*

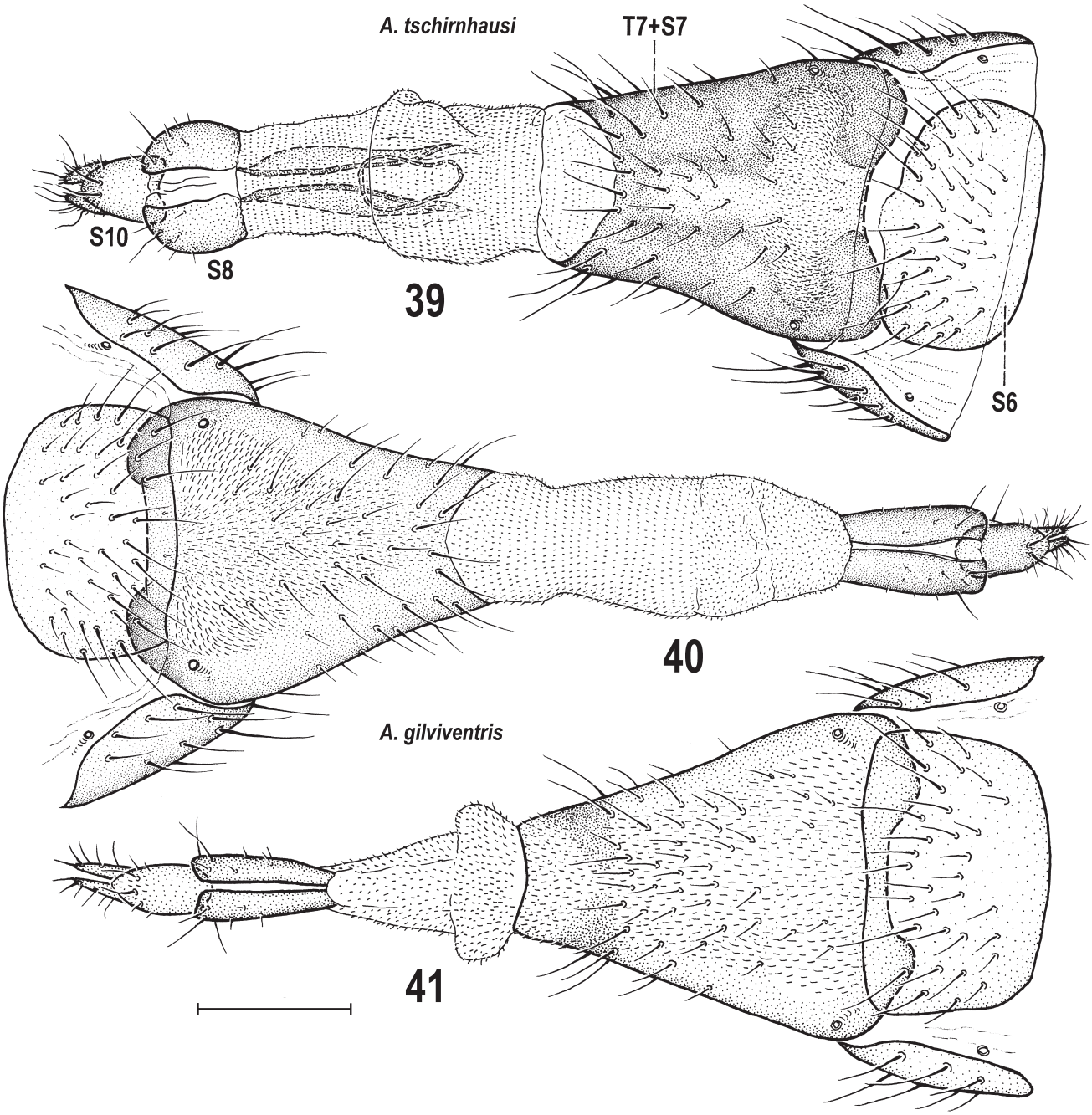

Figs 39–41. *Anthomyza* species, females, postabdomen ventrally. 39 – *A. tschirnhausi* Roháček, 2009, paratype (Kamchatka); 40–41 – *A. gilviventris* Roháček & Barber, 2016: 40 – paratype, Ontario; 41 – Sweden: Lögdeälven. Scale = 0.2 mm. Abbreviations: S – sternum, T7+S7 – tergosternum 7. Fig. 39 adapted from Roháček (2009: fig. 64), Fig. 40 from Roháček & Barber (2016: fig. 496, mirrored).

fluviatile and *Lysimachia thyrsiflora*) and *C. acuta* at the outlet of a small stream (see Fig. 44). In both these sedges, *A. gilviventris* was found together with *A. gracilis* Fallén, 1823 and *A. dissors* Collin, 1944, while *A. paraneglecta* Elberg, 1968 (1 ♂ only) was found only in *C. acuta*. No specimens of *A. gilviventris* were swept from tussocks of *C. nigra* ssp. *juncella* on the river shore or from the growth of *C. vesicaria* in the adjacent riverine forest. At the second site (at the river Öreälven), *A. gilviventris* was swept from *C. rostrata* growing in dense stands on the river bank where it was broader and sandy. In the third locality, at Lerfallet, only 2 ♀♀ were swept at a small creek, most probably on *Carex acuta* (not precisely recorded) on July 7, 2021.

Distribution. The species is widespread in the Nearctic Region, with numerous records from Canada (Alberta, British Columbia, Labrador, Manitoba, Newfoundland, Northwest Territories, Nova Scotia, Ontario, Quebec, Saskatchewan, Yukon) and the United States of America (Alaska, Colorado, Idaho, Michigan, Montana, New

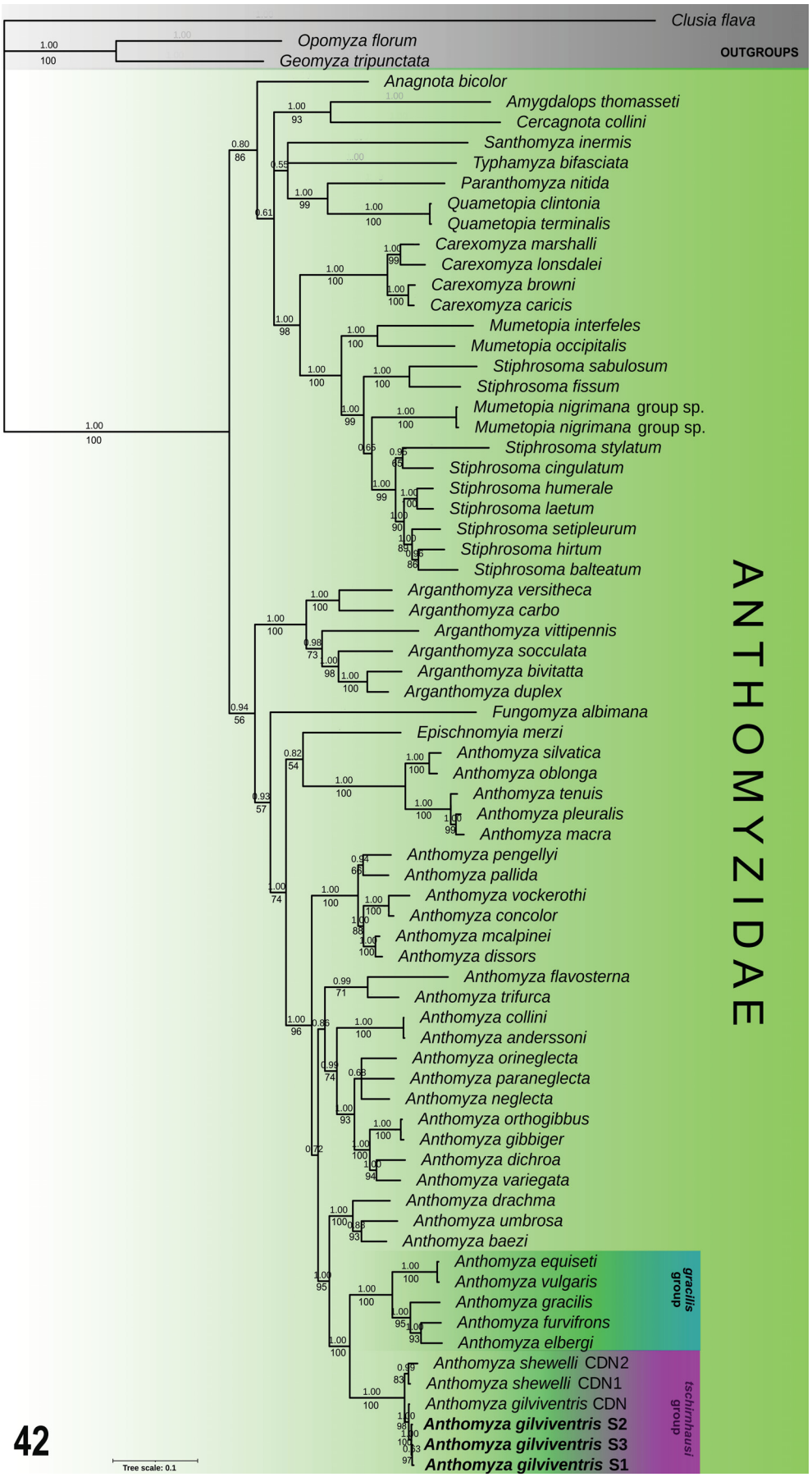

Fig. 42. Bayesian hypothesis for relationships of species of Anthomyzidae (with 6 specimens of the *A. tschirnhausi* group) based on DNA sequence data (12S, 16S, 28S, COI, COII, CytB, ITS2) representing 4568 characters. Numbers above nodes = posterior probability values if > 0.5, and below nodes = bootstrap support values for ML > 50. Abbreviations: CDN – specimens from Canada (Ontario), S – specimens from Sweden.

Figs 43–44. Habitat of *A. gilviventris* Roháček & Barber, 2016 in Sweden. 43 – general view of the habitat at Lögdeälven river bank; 44 – detail with growths of probable host plants in this locality. Photo by S. Hellqvist.

York, Washington, Wisconsin, Wyoming), see Roháček & Barber (2016). The above records of *A. gilviventris* from NE Sweden (see map, Fig. 45) are the first from the Palaearctic Region. This population is considered native (the species has surely been previously overlooked in northern Europe) and, consequently, *A. gilviventris* is an additional (one of only a few) naturally Holarctic species in the family Anthomyzidae. Formerly, only *Arganthomyza socculata* (Zetterstedt, 1847), *Stiphrosoma humerale* Roháček & Barber, 2005 and *S. sabulosum* (Haliday, 1837) were known to be distributed throughout the Holarctic Region (see Roháček & Barber 2005,

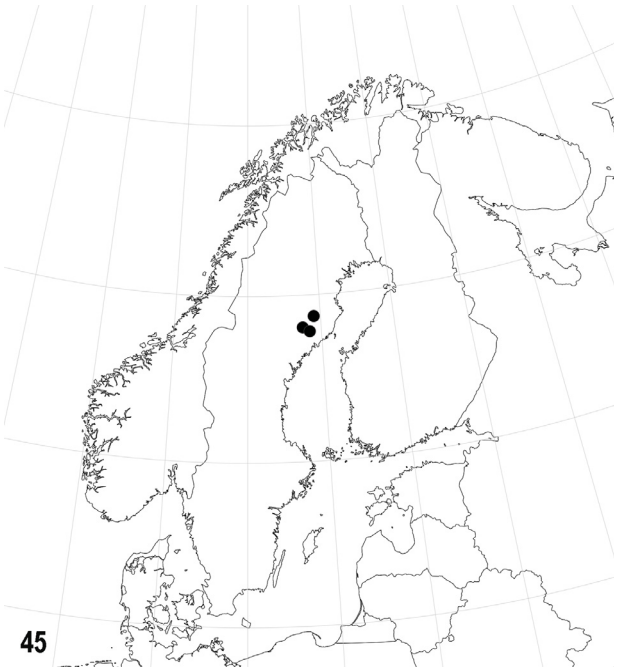

Fig. 45. Map of NW Europe with position of localities of *Anthomyza gilviventris* Roháček & Barber, 2016, in Sweden.

2016). However, the latter species could possibly be introduced in North America from Europe only in second half of 20th century (Roháček & Barber 2005).

Discussion and conclusions

(1) Morphological comparison of the Swedish *Anthomyza* specimens of the *A. tschirnhausi* group with those of *A. tschirnhausi* from Kamchatka and of *A. gilviventris* from Canada and the USA resulted in the conclusion that they are most similar to the typical (= yellow) form of *A. gilviventris*, including the colouration of the female abdomen (compare Fig. 2 and Roháček & Barber 2016: fig. 484). The less spinose apex of the filum of the distiphallus and the narrower female T10 of specimens from the Swedish population seem to be the only distinct differences from those of the Nearctic specimens. In the very similar and closely allied species, *A. tschirnhausi*, the apex of the filum has only three such spines (apart from the bicuspid apex), i.e. a number never found in Swedish specimens.

(2) Except for the size, shape and sclerotization of the transandrium (and its caudal process) and the gonostylus (which proved to be variable), all (albeit relatively small) differences in the male genitalia of *A. tschirnhausi* and *A. gilviventris* recognized by Roháček & Barber (2016) have been confirmed. In addition, both these species also differ in the presence (*A. gilviventris*) and absence (*A. tschirnhausi*) of a spine at the base of the membranous part of the saccus.

(3) The variability of the gonostylus and of the armature of the filum and saccus of the distiphallus (the latter previously recognized in *A. gilviventris* by Roháček & Barber 2016) has been described and illustrated. That of the gonostylus proved to be overlapping in both *A. tschirnhausi* and *A. gilviventris* while the number of spines on the apex of the filum and on the membranous part of the saccus (although variable) remain useful in separating these species.

(4) The differences in the female postabdominal structures (spermathecae, T7+S7, T8, S8) in these two species, previously recognized by Roháček & Barber (2016), have also been confirmed in specimens of *A. gilviventris* from Sweden. Both species also differ in the shape of T10 and S10 (narrower, more elongate in *A. gilviventris*) though T10 is particularly attenuated in Swedish specimens of *A. gilviventris* which differs from those from the Nearctic Region.

(5) The new molecular analyses (BI, ML) determined the specimens of Swedish origin as conspecific with *A. gilviventris* from Canada but also revealed a small genetic difference between them, with genetic distance of COI at 0.4–0.5%. The only other analysed species of the *A. tschirnhausi* group, viz., *A. shewelli*, proved to be a closely allied species, with a relatively small distance of COI from *A. gilviventris* (2.2–3.0%).

(6) The sister-group relationship of the *A. tschirnhausi* group and the *A. gracilis* group, recognized by previous analyses (Roháček & Barber 2016, Roháček et al. 2019), has been confirmed.

(7) Based on morphological characters, the Swedish population belongs to *A. gilviventris*, and *A. tschirnhausi* and *A. gilviventris* are still considered separate species. However, inasmuch as the morphological differences between these species are relatively small, we cannot exclude a possibility that they, in fact, belong to a single spe-

Table 2. Genetic pairwise distances of COI of the specimens of two species of the *A. tschirnhausi* group, using Kimura 2-parameter (K2P). Abbreviations: CDN – Canada (Ontario), S – Sweden.

	***Anthomyza gilviventris* CDN**	***Anthomyza gilviventris* S1**	***Anthomyza gilviventris* S2**	***Anthomyza gilviventris* S3**	***Anthomyza shewelli* CDN2**
***Anthomyza gilviventris* CDN**					
***Anthomyza gilviventris* S1**	0.4%				
***Anthomyza gilviventris* S2**	0.4%	0.0%			
***Anthomyza gilviventris* S3**	0.5%	0.2%	0.2%		
***Anthomyza shewelli* CDN2**	2.2%	2.7%	2.7%	3.0%	

cies, with the specimens from Kamchatka (*A. tschirnhausi*) representing the most aberrant population. Unfortunately, because of the absence of fresh material of *A. tschirnhausi* from Kamchatka, this hypothesis has not been tested by means of molecular methods.

Acknowledgements

It is an agreeable duty to express our sincere gratitude to all who kindly helped to improve the manuscript of this study: Kevin N. Barber (Sault Ste. Marie, Ontario, Canada) for valuable comments and language revision, Mikael Marberg (Umeå, Sweden) for photos of mounted adult specimens of *Anthomyza gilviventris* and Jan Ševčík (University of Ostrava, Czech Republic) for helpful suggestions on earlier drafts of the manuscript. The research of JR on Anthomyzidae was financially supported by the Ministry of Culture of the Czech Republic by institutional financing of long-term conceptual development of the research institution (the Silesian Museum, MK000100595).

References

BARBER K. N. & ROHÁČEK J. 2020: Revision of *Carexomyza* Roháček with descriptions of three new Nearctic species (Diptera: Anthomyzidae). *Arthropod Systematics & Phylogeny* **78**: 69–109.

CUMMING J. M. & WOOD D. M. 2009: 2. Adult morphology and terminology. Pp. 9–50. In: BROWN B. V., BORKENT A., CUMMING J. M., WOOD D. M., WOODLEY N. E. & ZUMBADO M. A. (eds): *Manual of Central American Diptera. Vol. 1*. NRC Research Press, Ottawa, 714 pp.

CUMMING J. M. & WOOD D. M. 2017: 2. Adult morphology and terminology. Pp. 89–133. In: KIRK-SPRIGGS A. H. & SINCLAIR B. J. (eds): *Manual of Afrotropical Diptera. Vol. 1. Introductory chapters and keys to Diptera families*. Suricata 4. SANBI Publishing, Pretoria, 425 pp.

GRIFFITHS G. C. D. 1972: *The phylogenetic classification of Diptera Cyclorrhapha with special reference to the structure of the male postabdomen*. Dr. W. Junk N.V., The Hague, 340 pp.

KATOH K. & STANDLEY D. M. 2013: MAFFT multiple sequence alignment software version 7: improvements in performance and usability. *Molecular Biology and Evolution* **30 (4)**: 772–780.

LETUNIC I. & BORK P. 2016: Interactive tree of life (iTOL) v3: an online tool for the display and annotation of phylogenetic and other trees. *Nucleic Acids Research* **44**: 242–245.

LONSDALE O. 2020: Family groups of Diopsoidea and Nerioidea (Diptera: Schizophora) – definition, history and relationships. *Zootaxa* **4735 (1)**: 1–177.

McALPINE J. F. 1989: 116. Phylogeny and classification of the Muscomorpha. Pp. 1397–1518. In: McALPINE J. F. & WOOD D. M. (eds): *Manual of Nearctic Diptera*. Agriculture Canada Monograph No. 32, Vol. 3. Minister of Supply and Services Canada, Ottawa, vi + 1333–1581 pp.

ROHÁČEK J. 1998: Taxonomic limits, phylogeny and higher classification of Anthomyzidae (Diptera), with special regard to fossil record. *European Journal of Entomology* **95**: 141–177.

ROHÁČEK J. 2006: A monograph of Palaearctic Anthomyzidae (Diptera) Part 1. *Časopis Slezského Zemského Muzea, Opava* (A) **55 (Supplement 1)**: 1–328.

ROHÁČEK J. 2009: A monograph of Palaearctic Anthomyzidae (Diptera) Part 2. *Časopis Slezského Zemského Muzea, Opava* (A) **58 (Supplement 1)**: 1–180.

ROHÁČEK J. & BARBER K. N. 2005: Revision of the New World species of *Stiphrosoma* Czerny (Diptera: Anthomyzidae). *Beiträge zur Entomologie*, Keltern **55 (1)**: 1–107.

ROHÁČEK J. & BARBER K. N. 2016: Nearctic Anthomyzidae: a monograph of *Anthomyza* and allied genera (Diptera). *Acta Entomologica Musei Nationalis Pragae* **56 (supplementum)**: 1–412.

ROHÁČEK J., PETRÁKOVÁ L. & TÓTHOVÁ A. 2019: Molecular phylogeny and timing of evolution of *Anthomyza* and related genera (Diptera: Anthomyzidae). *Zoologica Scripta* **48 (6)**: 745–760.

ROHÁČEK J. & TÓTHOVÁ A. 2021: *Mumetopia interfeles* sp. nov., a new species of Anthomyzidae (Diptera) occurring en masse in an urban grassy habitat in Chile: its taxonomy, phylogeny and biology. *European Journal of Taxonomy* **731**: 135–158.

RONQUIST F., TESLENKO M., MARK P. van der, AYRES D. L., DARLING A., HÖHNA S., LARGET B., LIU L., SUCHARD M. A. & HUELSENBECK J. P. 2012: MrBayes 3.2: efficient Bayesian phylogenetic inference and model choice across a large model space. *Systematic Biology* **61 (3)**: 539–542.

STAMATAKIS A. 2014: RAxML Version 8: a tool for phylogenetic analysis and post-analysis of large phylogenies. *Bioinformatics* **30 (9)**: 1312–1313.

TAMURA K., STECHER G. & KUMAR S. 2021: MEGA11: molecular evolutionary genetics analysis version 11. *Molecular Biology and Evolution* **38**: 3022–3027.

ZATWARNICKI T. 1996: A new reconstruction of the origin of eremoneuran hypopygium and its implications for classification (Insecta: Diptera). *Genus* **7 (1)**: 103–175.